


FULL PAPER

Open Access



Quasi-6-day wave effects in ionospheric E and F region during the recent solar maximum 2014–2015

Yi Liu, Qiong Tang, Guanyi Chen, Zhuangkai Wang and Chen Zhou* 

Abstract

We show the statistical characteristics of quasi-6-day wave (Q6DW) absolute amplitude in foE and foF_2 during 2014–2015 by using six ionosondes at different latitudes. The results show that foE perturbations maximized at mid-latitudes during equinoxes, and the maximum amplitude of Q6DW in foF_2 occurred near the northern crest of equatorial ionospheric anomaly (EIA). In addition, the absolute amplitude of Q6DW in foF_2 increased with increasing solar activity. Our observations suggest that the dissipative Q6DW-like oscillations in the lower thermosphere may cause variations in the thermospheric neutral density via mixing effect and further result in foE disturbances in Q6DW events. Furthermore, the E region wind dynamo could also be modulated by the 6-day wave, thus leading to the disturbances in vertical plasma velocity via $\mathbf{E} \times \mathbf{B}$ drifts and F region electron density. Our observational investigation provides evidence of thermosphere–ionosphere coupling in the mid- and low-latitude region.

Keywords: Quasi-6-day wave, Absolute amplitude in foE and foF_2 , Thermosphere–ionosphere coupling

Introduction

As a significant oscillation in the middle atmosphere, planetary waves (PWs) from lower atmosphere have been investigated over the past several decades (Madden and Julian 1972; Riggins et al. 2006; Chang et al. 2010; Gu et al. 2013; Onohara et al. 2013). The westward propagating quasi-6-day wave (Q6DW) with period of 5–7 days, is one of the most prominent traveling PWs in the mesosphere–lower thermosphere (MLT) region. Previous studies have revealed the effect of Q6DW on the wind and temperature in the MLT region by both ground-based and space-based instruments (Rodgers 1976; Venne 1989; Talaat et al. 2001, 2002; Liu et al. 2004; Garcia et al. 2005; Sridharan et al. 2008; Gan et al. 2015; Gu et al. 2018). Study of Q6DW in winds by using Upper Atmosphere Research Satellite/High Resolution Doppler Imager (HRDI) data was shown in Wu et al. 1994.

Their results illustrated that the maximum occurrence of Q6DW occurred during equinoxes in the equatorial and mid-latitude region in zonal and meridional winds, respectively. Gan et al. (2015) also presented the morphology of Q6DW in Thermosphere, Ionosphere, Mesosphere Energetics and Dynamics Doppler Interferometer (TIDI) horizontal wind and Sounding of the Atmosphere using Broadband Emission Radiometry (SABER) temperature data during 2002–2007. These global distributions of Q6DW occurrence presented in Gan et al. (2015) showed similar characteristics of Q6DW in the MLT region. Numerous research results have proposed that these seasonal variations of Q6DW response in the MLT region which reached a maximum during equinoxes were determined by background wave source, mean wind structure, baroclinic/barotropic instability, and critical layers of the wave (Meyer and Forbes 1997; Liu et al. 2004).

Recent studies have investigated the effect of Q6DW on the ionosphere by thermosphere–ionosphere coupling, which was generally attributed to the nonlinear

*Correspondence: chenzhou@whu.edu.cn
Department of Space Physics, School of Electronic Information, Wuhan University, Wuhan, China

interaction between tide and Q6DW and the modulation of E region dynamo due to wind disturbances in the MLT region (Miyoshi 1999; Gu et al. 2014, 2018; Gan et al. 2016, 2017; Forbes and Zhang 2017; Yamazaki, 2018). Pedatella et al. (2012) and Forbes and Zhang (2017) have proposed that strong Q6DW–tide nonlinear interactions could produce secondary waves that vertically propagated into the E region. By using the Thermosphere–Ionosphere–Mesosphere Electrodynamics General Circulation Model (TIME-GCM), Gan et al. [2016] suggested that the zonal electric field in the equatorial E layer could be modulated by neutral wind perturbations due to Q6DW in the MLT region, which was confirmed in the work shown in Yamazaki et al. (2018) based on observations from Challenging Minisatellite Payload (CHAMP) and Swarm satellites. Yamazaki (2018) investigated the characteristics of Q6DW in total electron content (TEC) in the low-latitude and equatorial region over a solar cycle. Wave amplitude peaks appeared in equinoxes which agreed with those observed in neutral wind and temperature in the MLT region. Gu et al. (2018) further analyzed the characteristics of Q6DW in TEC and horizontal wind in the MLT region. They suggested that polarization electric fields modulated by zonal wind perturbations in the equatorial E region could affect daytime plasma velocity by $E \times B$ drift, which eventually resulted in Q6DW-like oscillations in TEC in the equatorial ionospheric anomaly (EIA) region via the equatorial fountain effect. Furthermore, the dissipation of PWs in the MLT region may also play a significant role in the vertical coupling between thermosphere and ionosphere. Based on multiple observations, Yamazaki et al. 2020 revealed 6-day variations simultaneously in the equatorial electrojet, F-region electron density, and TEC during the September 2019, which were attributed to the Q6DW simultaneously observed in the lower atmosphere. Yue and Wang (2014) first investigated the PWs-induced variations in the thermosphere/ionosphere using the TIME-GCM and suggested that mixing effects caused by PWs could lead to the changes of both O/N_2 ratio and TEC. The theoretical results were later confirmed by recent work based on satellite observations Gan et al. 2015. They showed the reduction of O/N_2 ratio and F_2 layer electron density during Q6DW events.

The 6-day variations in the critical frequency of F_2 layer (foF_2) have been studied in the past several decades (Laštovička 1996; Laštovička and Mlch 1996; Laštovička 2006a). Laštovička et al. (2003, 2006b) investigated the planetary wave type oscillations in foF_2 by using ionosonde observations. These results presented that there was an obvious quasi-6-day oscillation amplitude in foF_2 . Altadill and Apostolov [2003] suggested the 6-day variations in foF_2 were attributed

to the planetary wave activity in the MLT region. Laštovička and Mlch [1996] presented that the 6-day variations in foF_2 have also distinct seasonal and solar activity variations. These results showed that the quasi-6-day oscillation amplitude in foF_2 reached a minimum during the solar minimum in summer. Although there are many reports on 6-day variations of foF_2 in the context of vertical coupling by the Q6DW, a statistical analysis about Q6DW effects on the critical frequency of E layer (foE) has not been reported yet. By using ionosonde observations at different latitude region during 2014–2015, the statistical results of 6-day variations in foE and foF_2 are first presented in this study. The main objective of this work is to study the effect of Q6DW on ionospheric E and F layer by thermosphere–ionosphere coupling.

Data and methods

In this present study, the ionograms are obtained from January 2014 to December 2015, which is the most recent solar maximum period. The ionosondes are located at Guam (13.62°N, 144.86°E, dip angle 12.65°), Sanya (19.40°N, 109.13°E, dip angle 27.12°), Wuhan (30.50°N, 114.40°E, dip angle 46.54°), Beijing (40.30°N, 116.20°E, dip angle 59.18°), Mohe (52.00°N, 122.52°E, dip angle 69.73°), and Yakutsk (62.00°N, 129.60°E, dip angle 76.46°). The geographic locations are presented in Fig. 1. The ionograms are routinely recorded every 15 min at all stations, which are automatically scaled by the computer routine automatic real-time ionogram scaler with true height analysis (Reinisch et al. 2009). The ionospheric parameters, namely, foE and foF_2 are utilized for studying Q6DW effects on the ionosphere.

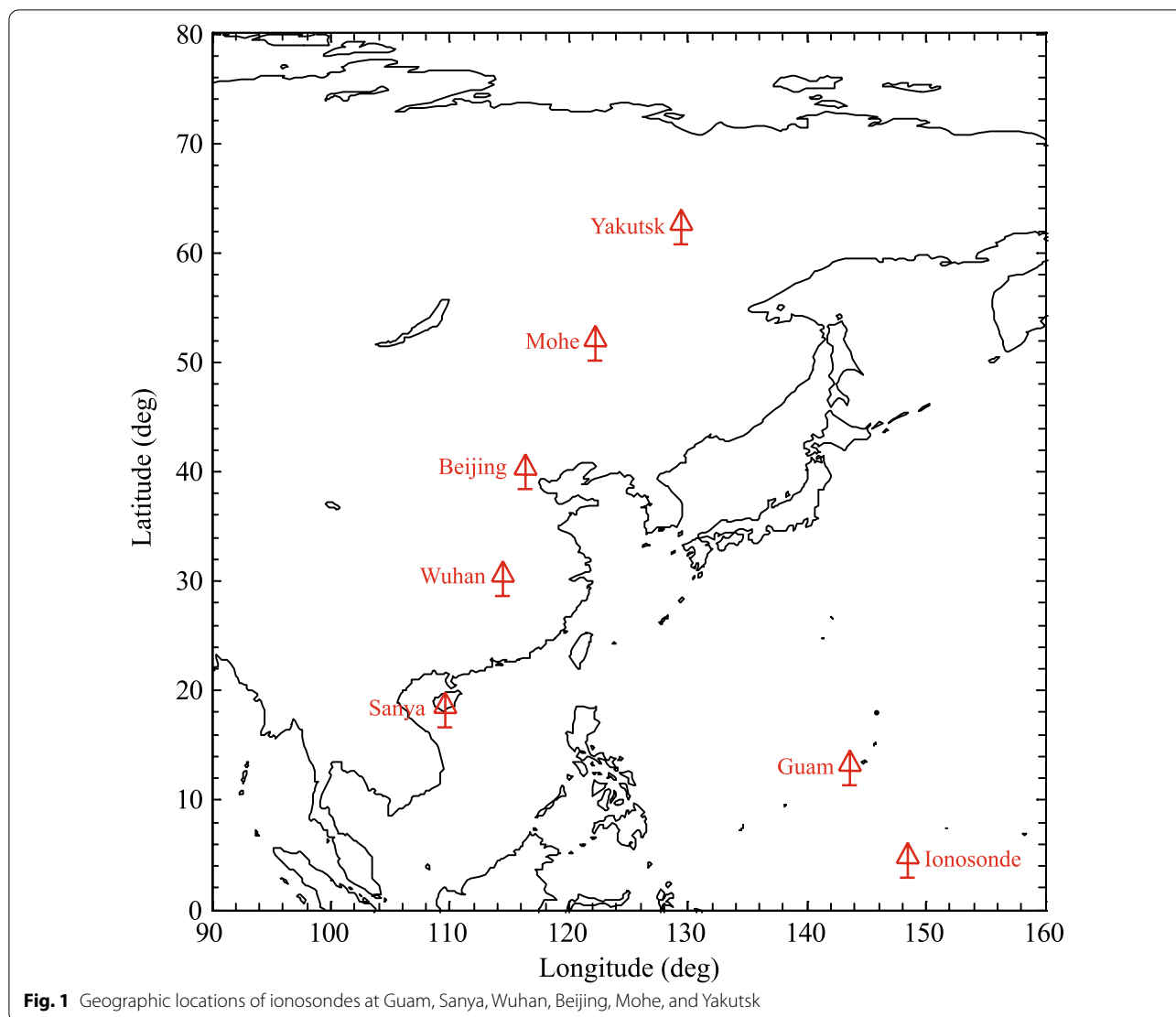
To obtain the information of wave in foE and foF_2 , the least square fitting model is adopted in the following formula within a 20-day running window at a 1-day time step:

$$y = A + B \cos \left[2\pi \left(\frac{t_d + t_u}{T} \right) \right] + C \sin \left[2\pi \left(\frac{t_d + t_u}{T} \right) \right] \quad (1)$$

where A represents the background value; T represents the period of wave in days; t_d represents the day of the year; t_u represents the universal time in days; and B , C represent the coefficient of the cosine and sine term, respectively. The amplitude of wave y_{wave} is written as:

$$y_{wave} = \sqrt{B^2(T) + C^2(T)}. \quad (2)$$

In this study, the parameters A , B , and C are calculated separately at different local times. The period T is considered with ranges of 4–8 days by increments of 0.125 day.



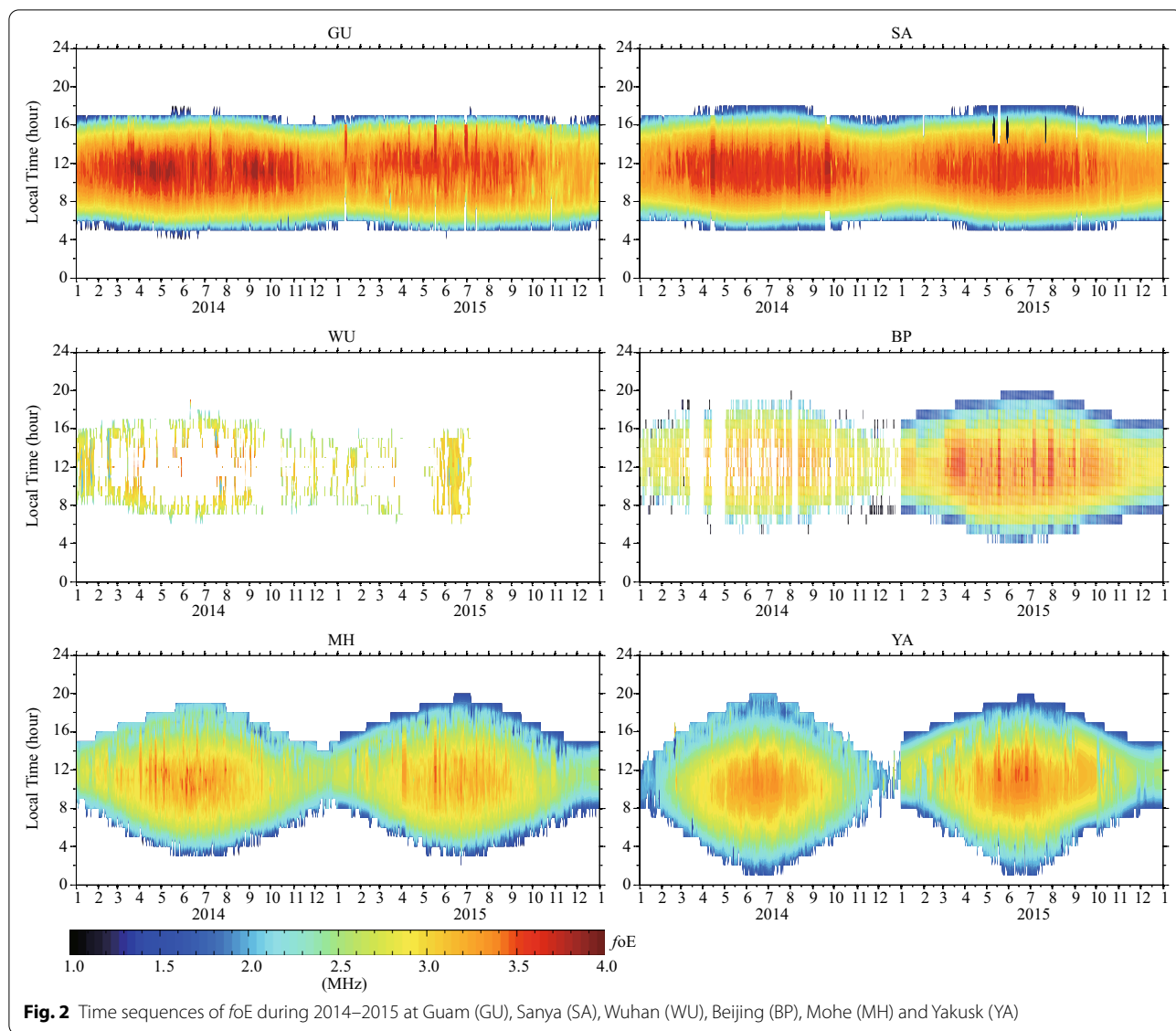
Results

Figure 2 presents the time series of f_oE during 2014–2015 at six stations with 1-h time resolution. There were serious data shortages at Wuhan in 2014–2015 and at Beijing in 2014 in Fig. 2. The maximum value of f_oE occurred at local noon in June solstice and minimum appeared in December solstice. f_oE value was greater at low-latitudes than that at middle-latitudes. Figure 3 shows the time series of f_oF_2 during 2014–2015. f_oF_2 peaks were observed during 12:00–18:00 LT in equinoxes at Guam and Sanya near the northern crest of EIA due to the equatorial fountain effect. In addition, the value of f_oF_2 increased with increasing solar activity ($F_{10.7} \approx 146$ in 2014 and $F_{10.7} \approx 118$ in 2015). It should be noted that there is a secondary maximum in f_oF_2 occurring around local midnight during

the equinoxes occurring at all stations equatorward of Beijing. The reason may be attributed to the enhanced electric field (Liu et al. 2013; Zhao et al. 2008).

The spectrum of f_oE at 12:00 LT at all stations in 2014 is presented in Fig. 4, except for Wuhan and Beijing due to data shortage. f_oE disturbance amplitude with period of ~ 6.5 days reached a maximum with about 0.2 MHz at Mohe in April, which indicates that there was a prominent Q6DW event in MLT region at Mohe during Spring. Furthermore, somewhat weaker disturbance in f_oE with period of 4.5–7.5 days was also observed at GU station during October, at SA station during March and October, at MH station during July and November and at YA station during November, respectively.

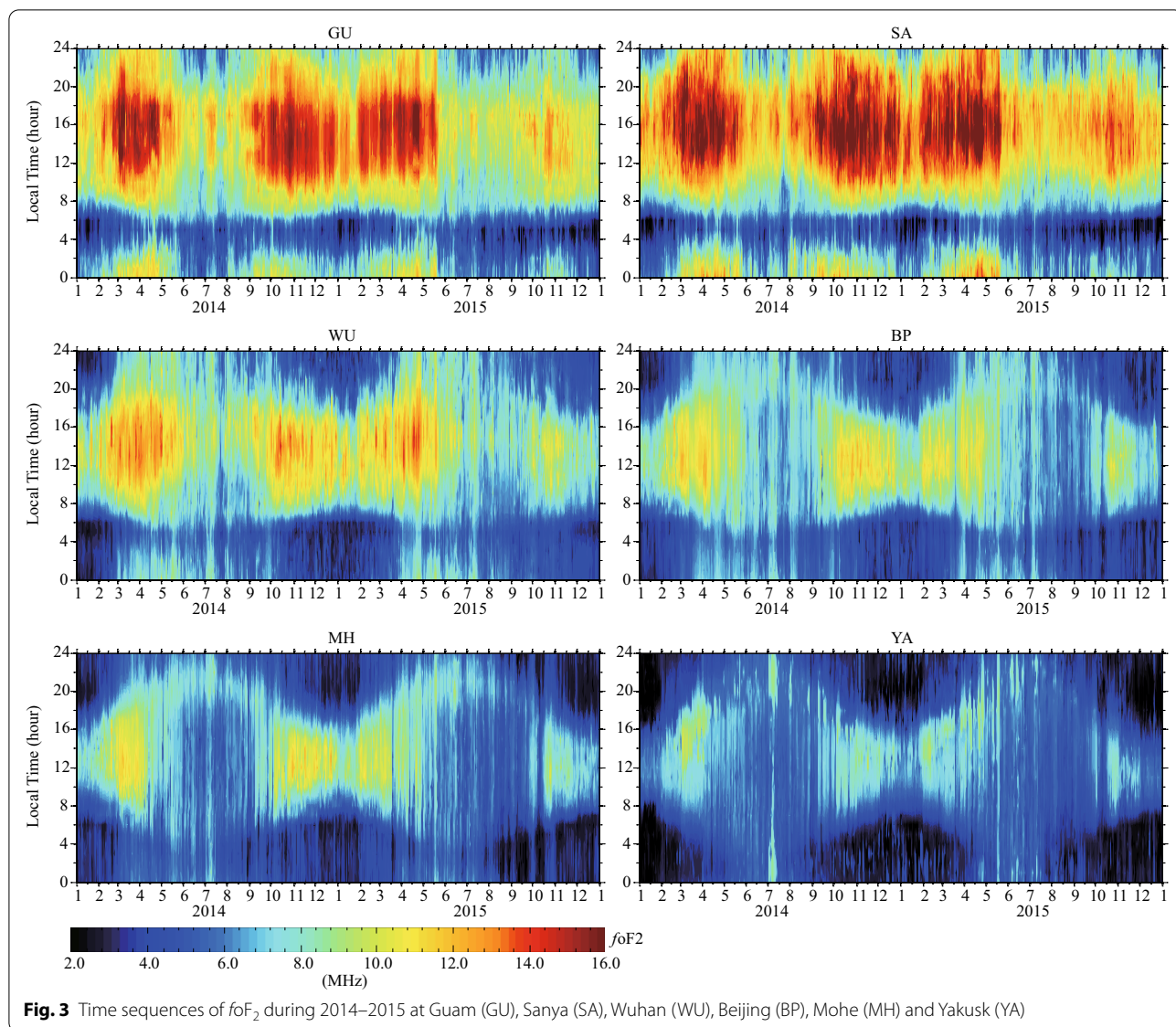
Figure 5 illustrates the f_oF_2 spectrum during 2014 at a fixed local time of 12:00 LT, which was clearly



dominated by a PW with period of ~ 6 days. The maximum amplitude of Q6DW in foF_2 occurred during April and November at all stations. The strongest absolute response in foF_2 appeared near the northern crest of EIA (GU and SA stations) with a maximum amplitude of ~ 1.4 MHz which accounted for $\sim 8\%$ of background foF_2 . Our results suggest that the latitude–season variations of Q6DW amplitude in foF_2 agreed well with the morphology of background foF_2 . Furthermore, compared to the large variation in Q6DW periods seen in foE in Fig. 4, the Q6DW periods in foF_2 are all quite similar for all events observed at all the stations. It should be noted that somewhat weaker disturbance in foF_2 with period of 5–7 days was also observed at all stations during summer (June, July and August). The

reason may be that foF_2 reached a minimum at all stations during summer, resulting in the weaker absolute response in foF_2 at all stations during summer.

The morphology of spectrum in foE at 12:00 LT at all stations in 2015 is shown in Fig. 6, except for Wuhan due to data shortage. Similar characteristics of Q6DW in foE are also found in Fig. 6. The maximum amplitude of Q6DW in foF_2 with period of ~ 7.0 days occurred during May at Mohe. Furthermore, somewhat weaker disturbance in foE with period of 4.5–7.5 days was also observed at GU station during November, at SA station during March and September, at BP station during September, at MH station during February and at YA station during April and October, respectively. Similar temporal and spatial distribution of Q6DW in



foF_2 in 2015 is also found in Fig. 7. Q6DW amplitude in foF_2 reached a maximum at GU and SA stations during equinoxes. Compared to the morphology of Q6DW in foF_2 during 2014 in Fig. 5, the weaker amplitude of Q6DW in foF_2 during 2015 may reveal the influence of solar activity, which was consistent with previous studies [e.g., Yamazaki 2018].

Figure 8 shows the local time versus month structures of Q6DW in foF_2 during 2014. In this study, the maximum amplitude of PWs with period of 5–7 days was adopted as the amplitude of Q6DW at different local time. Amplitude peaks were observed around 12:00–18:00 LT in the northern EIA crest region (at GU and SA stations) during equinoxes, which agreed well with the ionospheric fountain effect. The maximum

amplitude of Q6DW was ~ 1.5 MHz at Sanya at 16:00 LT, while amplitude reached minima during 06:00–08:00 LT. At the mid-latitude region, the absolute amplitude decreased with increasing latitude. Similar variations of Q6DW amplitude in 2015 are also shown in Fig. 9.

Discussion

In the above analysis, we mainly investigated the statistical features of Q6DW in foE and foF_2 based on 2014–2015 data set obtained by six ionosondes in different latitude region. The general characteristics of Q6DW were basically similar to previous studies (Gu et al. 2018, Yamazaki 2018). Our results have suggested

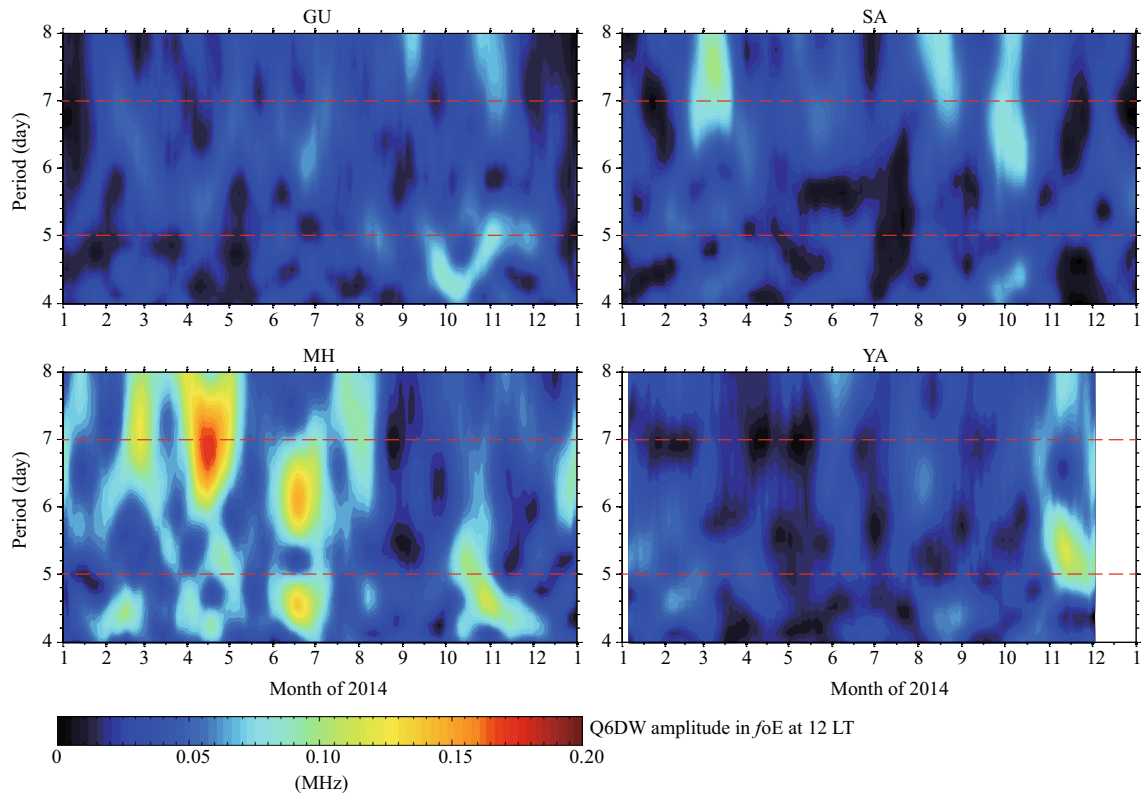


Fig. 4 The time variations of the foE spectrum at 12:00 LT during 2014 at Guam (GU), Sanya (SA), Wuhan (WU), Beijing (BP), Mohe (MH) and Yakusk (YA)

that the thermosphere–ionosphere coupling may be considered as the main reason for the effect of Q6DW on ionosphere.

In our reported results, the maximum amplitude of Q6DW in foE occurred at Mohe in equinoxes during 2014–2015. The generation mechanism of E region may help understand foE perturbations due to Q6DW in the MLT region. Daytime E layer at mid-latitudes is mainly produced in the ionization process of neutral O₂ by solar EUV radiation (Kelley 2009). Following Ivanov-Kholodny and Nusinov 1979, the expression of foE is given as follows:

$$\begin{aligned}
 f \text{ oE} &\propto (q_m/\alpha'_m)^{0.25} \\
 q_m/\alpha'_m &= \frac{I_\infty \sigma^i \cos \chi}{\alpha'_m H \sigma^a e},
 \end{aligned}
 \tag{3}$$

where q_m and α'_m are the maximum ionization rate and effective dissociative recombination coefficient in the E layer, respectively. I_∞ is the incident ionizing flux. σ^i and σ^a are the ionization and absorption cross sections. χ is the solar zenith angle. H is the O₂ scale height. e is elementary charge. According to Eq. (3), the variations of q_m , I_∞ , σ^i , σ^a , and χ depend on local time and solar

activity. Thus, we propose that the morphology of Q6DW in foE may be explained by the variations of α'_m or H during Q6DW events.

Ion compositions in the daytime mid-latitude E region are dominated by NO⁺ and O₂⁺ (Kelley 2009). Danilov (1994) and Danilov and Smirnova (1997) have suggested that α'_m depended on the NO⁺/O₂⁺ ratio, which was mainly controlled by [NO] concentration in the E region. In our cases, the maximum amplitude of Q6DW in foE was ~0.2 MHz which accounted for ~6% of background value. According to incoherent scatter radar observations, Mikhailov et al. (2007) proposed that 5% variations in foE may need the changes with a factor of 8–10 in [NO], which were impossible for the quiet daytime mid-latitude E region. Therefore, we suggest that the effect of α'_m variations during Q6DW events on foE disturbances could be neglected.

The effect of scale height H variations on foE changes has been studied by previous researches (Ivanov-Kholodny and Nusinov 1979; Mikhailov 1983; Nusinov 1988; Rishbeth 1990; Mikhailov et al. 2017). Mikhailov (1983) proposed that foE variations due to H variations were more likely to be induced by neutral particles vertical motion rather than neutral temperature changes.

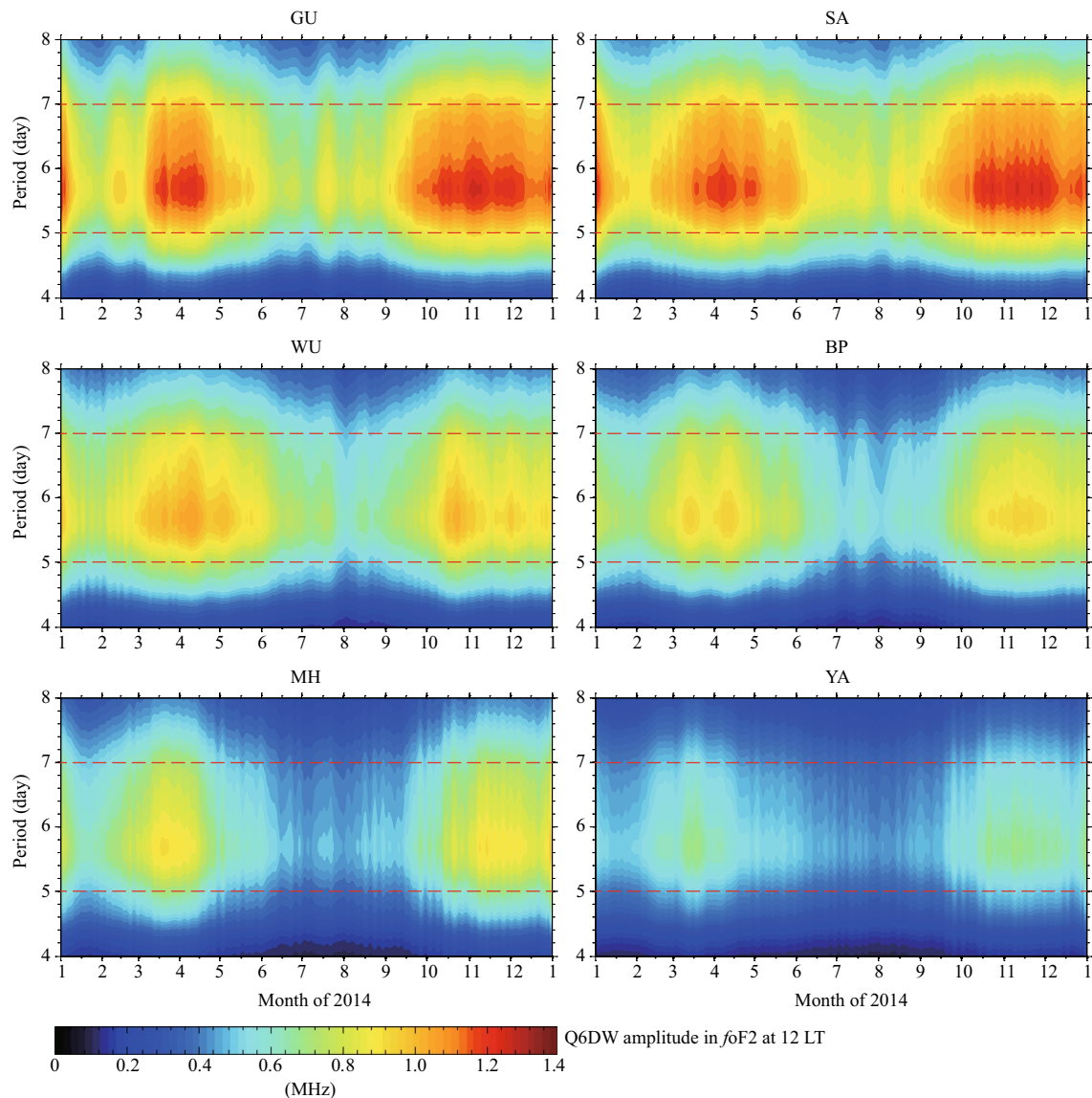


Fig. 5 The time variations of the foF_2 spectrum at 12:00 LT during 2014 at Guam (GU), Sanya (SA), Wuhan (WU), Beijing (BP), Mohe (MH) and Yakusk (YA). Dashed red lines represent the period of 5 and 7 days, respectively

They presented that the variations of neutral particle concentration by downwelling (upwelling) of neutral gas could cause a (an) reduction (increment) of $[O_2]$ effective scale height H , resulting in an (a) increment (reduction) of foE following Eq. (3). The changes of O, O_2 , and N_2 in the lower thermosphere during quasi-2-day wave (QTDW) events were shown in Yue and Wang (2014) using numerical simulation. They demonstrated that the extra meridional circulation induced by the dissipation of PWs could enhance the mixing of neutral composition, resulting in the changes of thermosphere/ionosphere. In addition, the reduction of O and the increase of O_2 and

N_2 shown in their work reached the maximum near 50° latitude at 120 km, which could induce the effective scale height H decrease and eventually cause foE maximum disturbances at mid-latitudes during QTDW events. In our observed results, Q6DW maximum amplitude in foE occurred at Mohe ($52.00^\circ N$, $122.52^\circ E$) during 2014–2015, which was agreement with the above analysis. Moreover, no significant 6-day variations in foE disturbances were observed at other stations. Therefore, we proposed that the effect of Q6DW on foE might be explained by mixing effect induced by the dissipation of Q6DW in the MLT region.

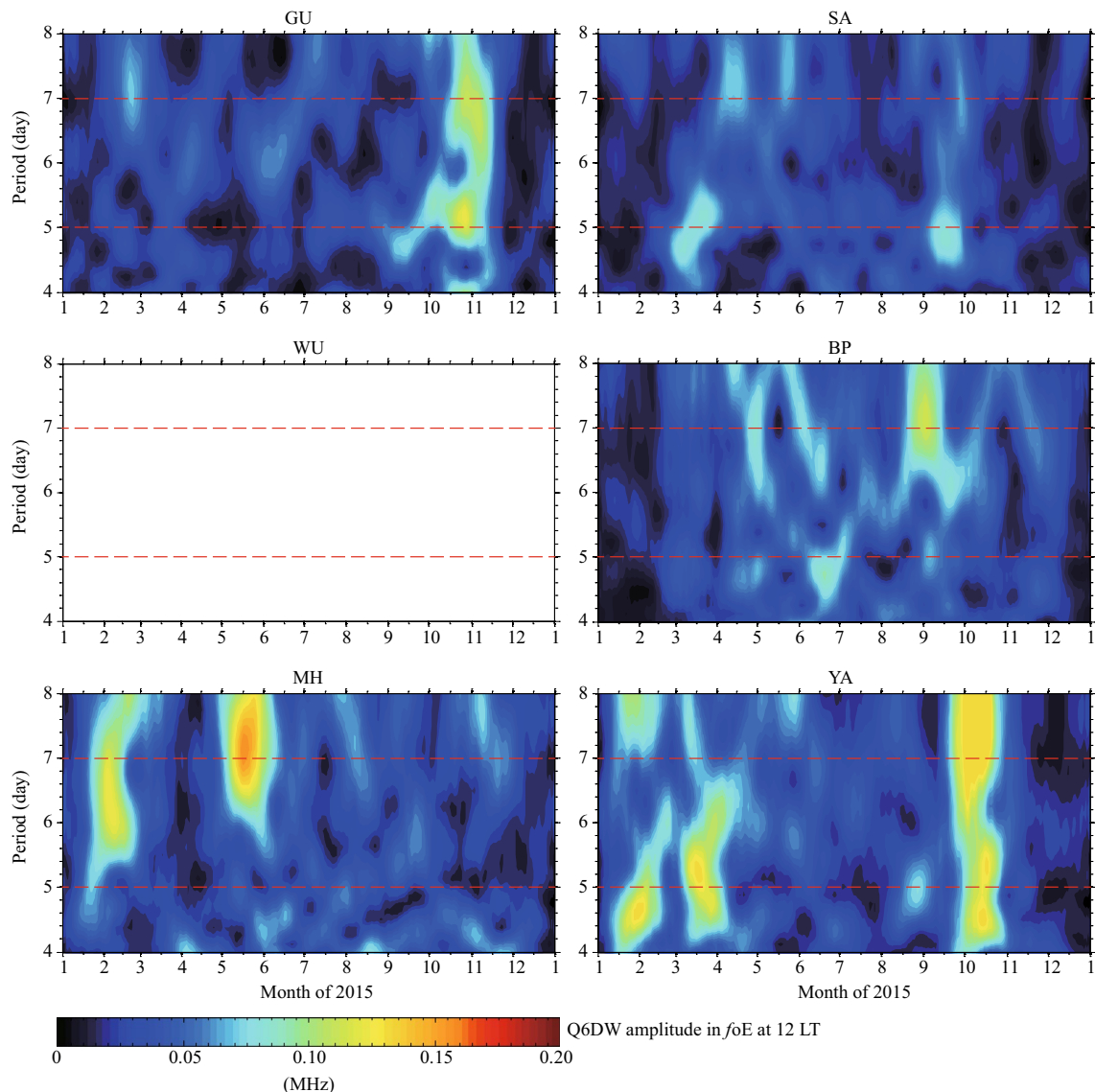


Fig. 6 The time variations of the foE spectrum at 12:00 LT during 2015 at Guam (GU), Sanya (SA), Wuhan (WU), Beijing (BP), Mohe (MH) and Yakusk (YA)

It should be noted that the period of foE disturbance is not strictly within 6 days, which varies from 4.5 days to 7.5 days. Liu et al. (2004) suggested that this phenomenon may be caused by the effect of Doppler shift. In addition, the large variation in Q6DW periods seen in foE could also be caused by ionospheric parameter foE measurement errors, which may be induced due to the presence of sporadic E layer (E_s). Kelley [2009] proposed that an enhanced metallic-ion layer (a factor of 2–5 in foE) is frequently observed in ionospheric E region in mid- and low-latitude regions. The high-density E_s could result in the measurement errors in foE, which could lead to

a deviation in the period of foE disturbance during the Q6DW events.

Our statistical results also presented that the latitude structures of 6-day oscillation in foF₂ reached a maximum near the northern crest of EIA, which indicated the effect of Q6DW on the equatorial fountain effect via modulating E region dynamo in the MLT region (Gan et al. 2016, 2018; Gu et al. 2018; Yamazaki 2018; Yamazaki et al. 2018). Liu et al. (2010) showed that zonal gradients of zonal and meridional wind perturbations from PWs could generate convergence/divergence of Pedersen and Hall currents, resulting in eastward polarized electric

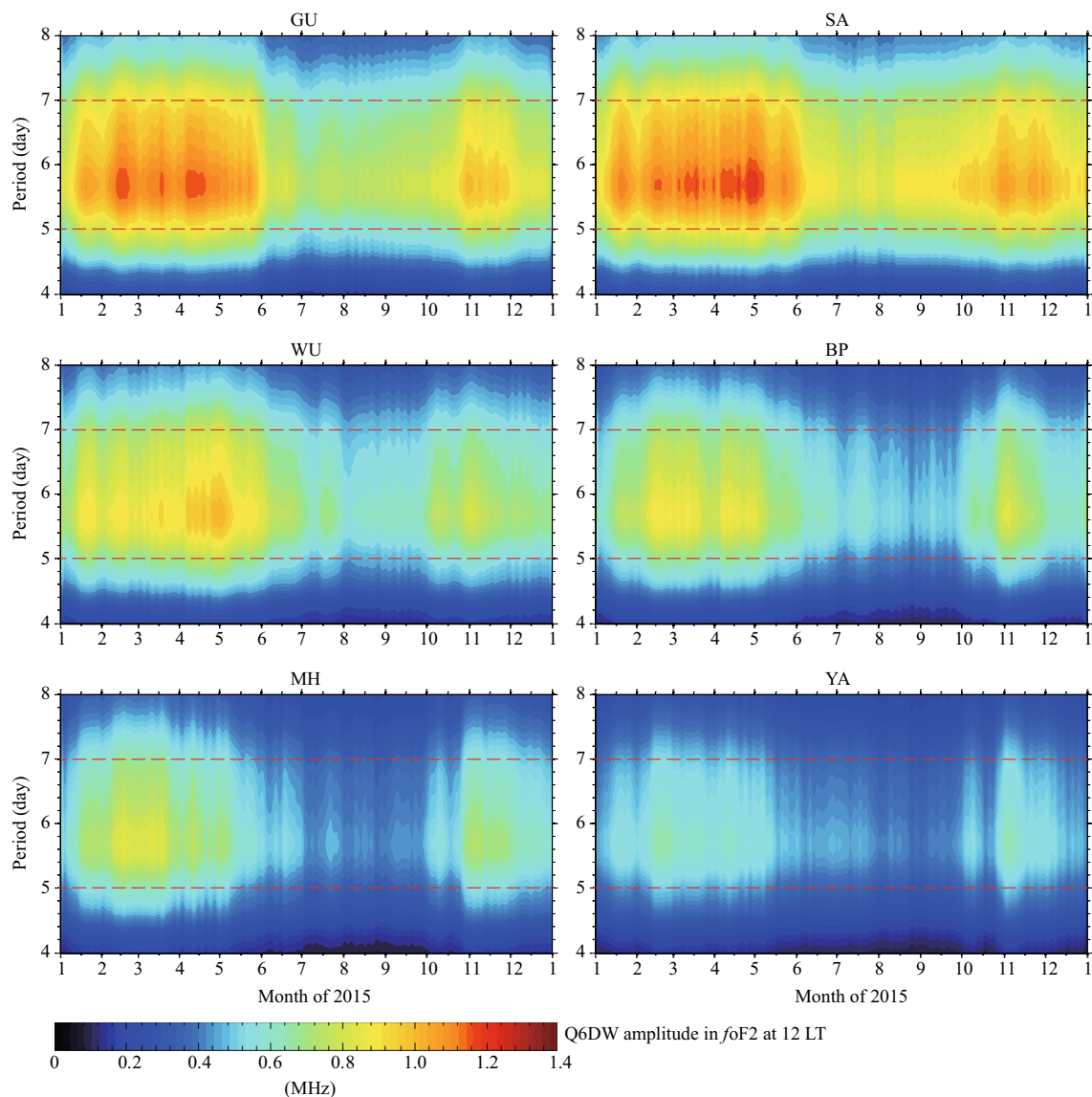


Fig. 7 The time variations of the foF_2 spectrum at 12:00 LT during 2015 at Guam (GU), Sanya (SA), Wuhan (WU), Beijing (BP), Mohe (MH) and Yakusk (YA)

fields and equatorial vertical ion drifts. According to the dynamo theory, the wind-driven eastward currents are given as follows:

$$\begin{aligned} J_x^P &= -\sigma_P v B \sin I, \\ J_x^H &= \sigma_H u B, \end{aligned} \tag{4}$$

where J_x^P and J_x^H are eastward Pedersen and Hall currents, respectively. σ_P and σ_H are Pedersen and Hall conductivities. u and v are zonal and meridional winds in the magnetic coordinates. B represents the geomagnetic field. I is the magnetic dip angle. From Eq. (4), it is found

that J_x^H is larger at magnetic low-latitude and equatorial region compared to J_x^P due to the finite dip angle. In addition, based on TIDI observations, zonal wind perturbations in the MLT region during Q6DW events were much stronger than those of meridional wind at low-latitude and equatorial region Gan et al. 2015. Therefore, we propose that the zonal wind component of Q6DW in the MLT region contributes more to foF_2 variations at low-latitude and equatorial region by thermosphere-ionosphere coupling.

Recent studies have presented that the nonlinear interaction between tide and Q6DW in the coupling process

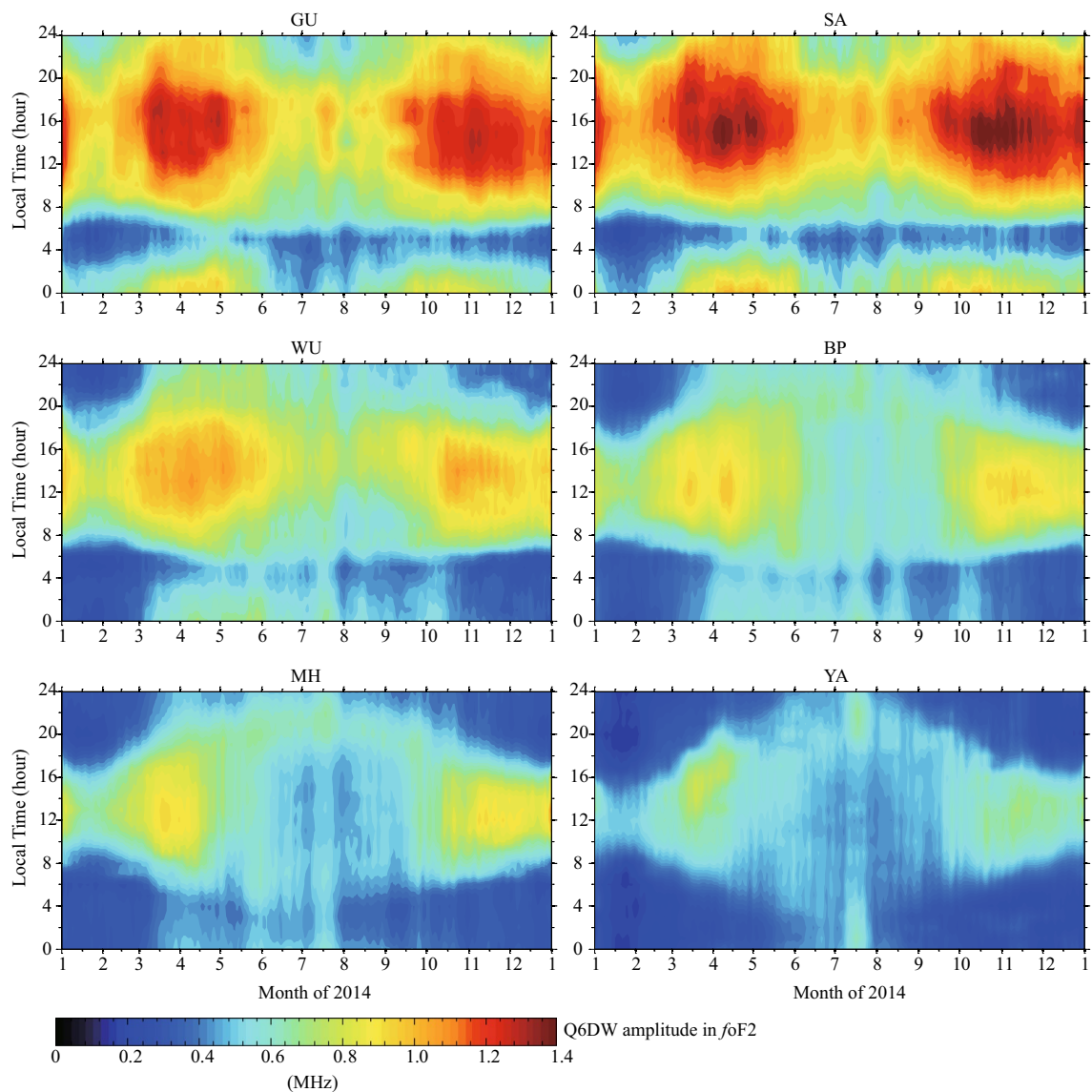


Fig. 8 Average amplitude of Q6DW ($s = 1$) in foF_2 during 2014 at Guam (GU), Sanya (SA), Wuhan (WU), Beijing (BP), Mohe (MH) and Yakusk (YA)

also resulted in the variations in the F region ionosphere, especially the diurnal and semidiurnal variability. In the recent modeling work, Gan et al. (2016) illustrated migrating diurnal and semidiurnal tidal disturbances in F region electron densities during Q6DW events. Their results suggested that short-term variability of F region electron densities may result from strong Q6DW–tide nonlinear interaction via thermosphere–ionosphere coupling. Similar conclusions were also shown in Liu et al. (2010) and Yue et al. (2016). Furthermore, mixing effect induced by the dissipation of Q6DW in the MLT region could cause not only foE variations, but also foF_2 changes. With the decreased O and increased O_2 and

N_2 propagating into the F region by molecular diffusion, O/N_2 ratio presented in Yue and Wang (2014) was decreased by about 16% and 20% near the ionospheric F_2 peak at low-latitudes and mid-latitudes. According to previous study, F_2 region electron density was proportional to O/N_2 ratio (Rishbeth 1998). Therefore, the reduced O/N_2 ratio could also produce the variations of foF_2 during Q6DW events.

Yamazaki 2018 presented the effect of solar activity on the absolute amplitude of Q6DW in TEC based on a long-term data set during 2004–2017. They showed that absolute amplitude at low-latitudes increased with increasing solar activity. In this work, we presented

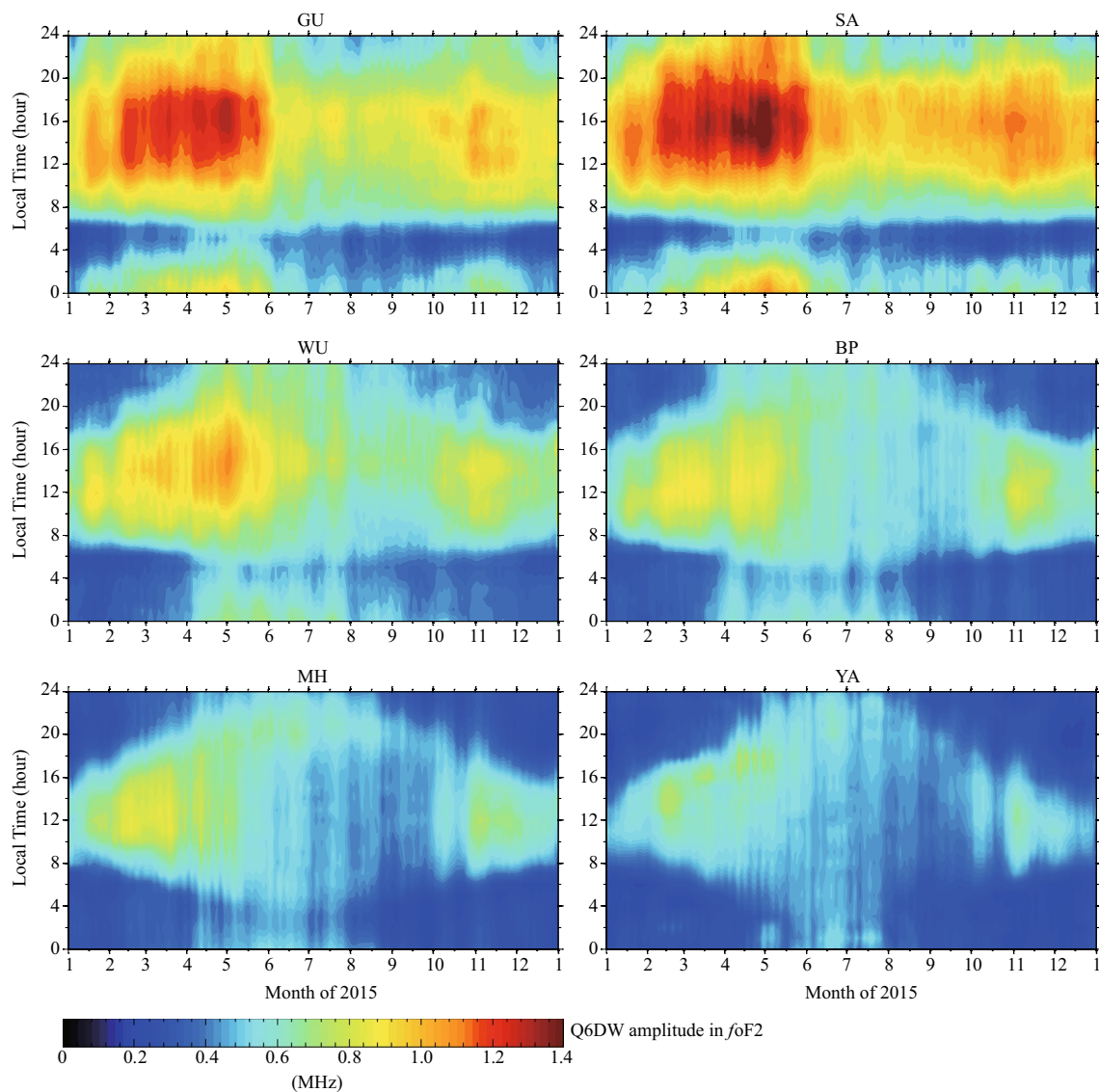


Fig. 9 Average amplitude of Q6DW ($s = 1$) in foF_2 during 2015 at Guam (GU), Sanya (SA), Wuhan (WU), Beijing (BP), Mohe (MH) and Yakusk (YA)

similar features of Q6DW absolute amplitude in foF_2 during 2014–2015. The weaker amplitude occurred in 2015 due to lower solar activity. Our study provides observational evidences of the solar activity dependence of absolute amplitude in foF_2 response to Q6DW from lower atmosphere.

Summary

In this work, we reported observations of six ionosondes during the most recent solar maximum 2014–2015. Morphology of Q6DW absolute amplitude in foE and foF_2 at different latitudes was investigated during this period. We also discussed the effects of Q6DW in the MLT

region on ionosphere via thermosphere–ionosphere coupling. The conclusions are summarized as follows:

1. In our statistical results, the maximum amplitude of Q6DW in foF_2 occurred around 12:00–18:00 LT in equinoxes near the northern EIA crest region. The absolute amplitude in foE reached the maximum in equinoxes at mid-latitudes. In addition, the solar activity dependence of absolute amplitude in foF_2 due to Q6DW was also shown in our study. These results were in agreement with previous studies.

2. It is suggested that the mixing effect induced by the dissipation of Q6DW in the MLT region could change E region neutral composition and reduce effective scale

height H , which eventually caused foE disturbances during Q6DW events. Furthermore, equatorial zonal wind disturbances due to Q6DW in the MLT region could modulate E region dynamo and vertical plasma drifts, resulting in F region electron density changes in the northern crest of EIA via equatorial fountain effect. Our study proposes that the thermosphere–ionosphere coupling plays a key role in ionospheric variations due to Q6DW from lower atmosphere.

Key points

- Q6DW signatures in foE and foF_2 are simultaneously examined using an array of ionosondes.
- The latitudinal changes of Q6DW in foE and foF_2 may be caused by mixing effects and modulation of E region dynamo due to PWs, respectively.
- Thermosphere–ionosphere coupling may play a significant role in the effect of Q6DW on ionosphere in the mid- and low-latitude region.

Abbreviations

Q6DW: Quasi-6-day wave; EIA: Equatorial ionospheric anomaly; PWs: Planetary waves; MLT: Mesosphere–lower thermosphere; TIDI: Thermosphere, Ionosphere, Mesosphere Energetics and Dynamics Doppler Interferometer; SABER: Sounding of the Atmosphere using Broadband Emission Radiometry; TIME-GCM: Thermosphere–Ionosphere–Mesosphere Electrodynamics General Circulation Model; CHAMP: Challenging Minisatellite Payload; TEC: Total electron content; QTDW: Quasi-2-day wave.

Acknowledgements

We acknowledge the use of ionosonde data from Digital Ionogram Data Base (DIDBase).

Authors' contributions:

YL performed data processing and statistical analysis on Q6DW absolute amplitude in foE and foF_2 and drafted the manuscript. GC, QT and ZW elaborated on the processing of foE and foF_2 data and supervised all the work of CZ and YL. GC CZ and YL participated in the discussion and interpretation of the statistical results obtained. All authors have read and approved the final manuscript.

Funding

This work was supported by the National Natural Science Foundation of China (NSFC grant Nos. 41574146, 41774162, 42074187), the National Key R&D Program of China (Grant No. 2018YFC1503506), the foundation of National Key Laboratory of Electromagnetic Environment (Grant No. 6142403180204), and by Excellent Youth Foundation of Hubei Provincial Natural Science Foundation (Grant No. 2019CFA054).

Availability of data and materials

The data that support the findings of this study are available upon request from the corresponding author.

Ethics approval and consent to participate

Not applicable.

Consent for publication

Not applicable.

Competing interests

The authors declare that they have no competing interests.

Received: 1 July 2020 Accepted: 19 November 2020

Published online: 11 December 2020

References

- Altadill D, Apostolov EM (2003) Time and scale size of planetary wave signatures in the ionospheric F region: Role of the geomagnetic activity and mesosphere/lower thermosphere winds. *J Geophys Res* 108(A11):1403. <https://doi.org/10.1029/2003JA010015>
- Chang LC, Palo SE, Liu HL, Fang TW, Lin CS (2010) Response of the thermosphere and ionosphere to an ultra-fast Kelvin wave. *J Geophys Res.* <https://doi.org/10.1029/2010JA015453>
- Danilov AD (1994) Ion chemistry of the lower thermosphere. *J Atmos Solar Terr Phys* 56:1213–1225. [https://doi.org/10.1016/0021-9169\(94\)90059-0](https://doi.org/10.1016/0021-9169(94)90059-0)
- Danilov AD, Smirnova NV (1997) Long-term trends of the ion composition in the E region. *Geomag Aeronom* 37(N4):35–40
- Forbes JM, Zhang XL (2017) The quasi-Q6DW and its interactions with solar tides. *Journal Geophy Res Space Phy* 122:4764–4776. <https://doi.org/10.1002/2017ja023954>
- Gan Q, Yue J, Chang LC, Wang WB, Zhang SD, Du J (2015) Observations of thermosphere and ionosphere changes due to the dissipative 65-day wave in the lower thermosphere. *Ann Geophys* 33(7):913–922. <https://doi.org/10.5194/angeo-33-913-2015>
- Gan Q, Wang WB, Yue J, Liu HL, Chang LC, Zhang SD, Du JA (2016) Numerical simulation of the 6 day wave effects on the ionosphere: Dynamo modulation. *J Geophys Res Space Phy* 121:10103–10116. <https://doi.org/10.1002/2016JA022907>
- Gan Q, Oberheide J, Yue J, Wang WB (2017) Short-term variability in the ionosphere due to the nonlinear interaction between the 6 day wave and migrating tides. *J Geophy Res Space Phys* 122:8831–8846. <https://doi.org/10.1002/2017ja023947>
- Gan Q, Oberheide J, Pedatella NM (2018) Sources, sinks, and propagation characteristics of the quasi 6-day wave and its impact on the residual mean circulation. *J Geophys Res Atmospheres* 123:9152–9170. <https://doi.org/10.1029/2018JD028553>
- Garcia RR, Lieberman R, Russell JM, Mlynczak MG (2005) Large-scale waves in the mesosphere and lower thermosphere observed by SABER. *J Atmospheric Sci* 62(12):4384–4399. <https://doi.org/10.1175/Jas3612.1>
- Gu SY, Li T, Dou XK, Wu Q, Mlynczak MG, Russell JM (2013) Observations of quasi-two-day wave by TIMED/SABER and TIMED/TIDI. *J Geophy Res Atmospheres* 118:1624–1639. <https://doi.org/10.1002/jgrd.50191>
- Gu S-Y, Liu HL, Li T, Dou XK, Wu Q, Russell JM (2014) Observation of the neutral-ion coupling through 6 day planetary wave. *J Geophys Res Space Phys* 119:10376–10383. <https://doi.org/10.1002/2014JA020530>
- Gu S-Y, Ruan H, Yang C-Y, Gan Q, Dou X, Wang N (2018) The morphology of the 6-day wave in both the neutral atmosphere and F region ionosphere under solar minimum conditions. *J Geophy Res Space Phys* 123:4232–4240. <https://doi.org/10.1029/2018JA025302>
- Ivanov-Kholodny GS, Nusinov AA (1979) Formation and dynamics of the daytime mid-latitude ionospheric E-layer [in Russian]. *Transactions of IAG* 37:128
- Kelley MC (2009) The Earth's ionosphere: Plasma physics and electrodynamics (International Geophysics Series), vol 43. Academic, San Diego, CA, USA
- Laštovička J (1996) Similarities in the variability of the lower ionosphere and foF_2 in the period range of 2–15 days. *Adv Space Res* 18(3):117–120. [https://doi.org/10.1016/0273-1177\(95\)00849-A](https://doi.org/10.1016/0273-1177(95)00849-A)
- Laštovička J, Mlch P (1996) Solar cycle effects on oscillations in the period range of 2–20 days in the F region of the ionosphere. *Ann Geofis* 39:783–790. <https://doi.org/10.4401/ag-4018>
- Laštovička J, Križan Š, P, & Novotná, D. (2003) Persistence of the planetary wave type oscillations in foF_2 over Europe. *Ann Geophys* 21:1543–1552. <https://doi.org/10.5194/angeo-21-1543-2003>
- Laštovička J (2006) Forcing of the ionosphere by waves from below. *J Atmos Solar Terr Phys* 68(3–5):479–497. <https://doi.org/10.1016/j.jastp.2005.01.018>

- Laštovička J, Šauli P, Križan P (2006) Persistence of the planetary wave type oscillations in mid-latitude ionosphere. *Annals Geophys.* <https://doi.org/10.4401/ag-3098>
- Liu HL, Talaat ER, Roble RG, Lieberman RS, Riggan DM, Yee JH (2004) The 65-day wave and its seasonal variability in the middle and upper atmosphere. *J Geophys Res* 109:D21112. <https://doi.org/10.1029/2004JD004795>
- Liu HL, Wang W, Richmond AD, Roble RG (2010) Ionospheric variability due to planetary waves and tides for solar minimum conditions. *J Geophys Res.* <https://doi.org/10.1029/2009JA015188>
- Liu L, Chen Y, Le H, Ning B, Wan W, Liu J, Hu L (2013) A case study of post-midnight enhancement in F-layer electron density over Sanya of China. *J Geophys Res Space Phys* 118:4640–4648. <https://doi.org/10.1002/jgra.50422>
- Madden RA, Julian PA (1972) Further evidence of global-scale 5-day pressure waves. *J Atmospheric Sci* 29(8):1464–1469. [https://doi.org/10.1175/1520-0469\(1972\)029%3C1464:FEOGSD%3E2.0.CO;2](https://doi.org/10.1175/1520-0469(1972)029%3C1464:FEOGSD%3E2.0.CO;2)
- Meyer CK, Forbes JM (1997) A 65-day westward propagating planetary wave: Origin and characteristics. *J Geophys Res* 102(26):173–178. <https://doi.org/10.1029/97JD01464>
- Mikhailov AV (1983) Possible mechanism for the in-phase changes in the electron densities in the ionospheric E and F2 regions. *Geomagn Aeron* 23:455–458
- Mikhailov AV, Depuev VH, Depueva AH (2007) Synchronous NmF2 and NmE daytime variations as a key to the mechanism of quiet-time F2-layer disturbances. *Ann Geophys* 25:483–493. <https://doi.org/10.5194/angeo-25-483-2007>
- Mikhailov AV, Perrone L, Nusinov AA (2017) A mechanism of midlatitude noontime foE long-term variations inferred from European observations. *J Geophys Res Space Physics* 122:4466–4473. <https://doi.org/10.1002/2017JA023909>
- Miyoshi Y (1999) Numerical simulation of the 5-day and 16-day waves in the mesopause region. *Earth Planets Space* 51:763–772
- Nusinov AA (1988) Deterministic model of mid-latitude and equatorial E-layer (Description and comparative characteristics of the accuracy) [in Russian]. *Ionosph. Researches* 44:94–97
- Onohara AN, Batista IS, Takahashi H (2013) The ultra-fast Kelvin waves in the equatorial ionosphere: Observations and modeling. *Annales Geophysique* 31(2):209–215. <https://doi.org/10.5194/angeo-31-209-2013>
- Pedatella NM, Liu HL, Hagan ME (2012) Day-to-day migrating and nonmigrating tidal variability due to the six-day planetary wave. *J Geophys Res* 117:A06301. <https://doi.org/10.1029/2012ja017581>
- Reinisch BW et al (2009) New Digisonde for research and monitoring applications. *Radio Sci.* <https://doi.org/10.1029/2008RS004115>
- Riggan DM, Liu HL, Lieberman RS, Roble RG, Russell JM III, Mertens CJ et al (2006) Observations of the 5-day wave in the mesosphere and lower thermosphere. *J Atmos Solar Terr Phys* 68(3–5):323–339. <https://doi.org/10.1016/j.jastp.2005.05.010>
- Rishbeth H (1990) A greenhouse effect in the ionosphere? *Planet Space Sci* 38:945–948. [https://doi.org/10.1016/0032-0633\(90\)90061-T](https://doi.org/10.1016/0032-0633(90)90061-T)
- Rishbeth H (1998) How the thermospheric circulation affects the ionospheric F2 layer. *J Atmos Solar Terr Phys* 60:1385–1402
- Rodgers CD (1976) Evidence for the five-day wave in the upper stratosphere. *J Atmospheric Sci* 33:710–711. [https://doi.org/10.1175/1520-0469\(1976\)033%3C0710:EFTFDW%3E2.0.CO;2](https://doi.org/10.1175/1520-0469(1976)033%3C0710:EFTFDW%3E2.0.CO;2)
- Sridharan S, Tsuda T, Nakamura T, Horinouchi T (2008) The 5–8-day Kelvin and Rossby waves in the tropics as revealed by ground and satellite-based observations. *J Meteorol Soc Jpn* 86(1):43–55. <https://doi.org/10.2151/jmsj.86.43>
- Talaat ER, Yee JH, Zhu X (2001) Observations of the 65-day wave in the mesosphere and lower thermosphere. *J Geophys Res* 106(20):715–723. <https://doi.org/10.1029/2001JD900227>
- Talaat ER, Yee JH, Zhu X (2002) The 65-day wave in the tropical stratosphere and mesosphere. *J Geophys Res* 107(D12):4133. <https://doi.org/10.1029/2001JD000822>
- Venne DE (1989) Normal-mode Rossby waves observed in the wavenumber 1–5 geopotential fields of the stratosphere and troposphere. *J Atmospheric Sci* 46:1042–1056. [https://doi.org/10.1175/1520-0469\(1989\)046%3C1042:NMRWOI%3E2.0.CO;2](https://doi.org/10.1175/1520-0469(1989)046%3C1042:NMRWOI%3E2.0.CO;2)
- Wu DL, Hays PB, Skinner WR (1994) Observations of the 5-day wave in the mesosphere and lower thermosphere. *Geophys Res Lett* 21(24):2733–2736. <https://doi.org/10.1029/94GL02660>
- Yamazaki Y (2018) Quasi-6-day wave effects on the equatorial ionization anomaly over a solar cycle. *J Geophys Res Space Phys* 123:9881–9892. <https://doi.org/10.1029/2018JA026014>
- Yamazaki Y, Stolle C, Matzka J, Alken P (2018) Quasi-6-day wave modulation of the equatorial electrojet. *J Geophys Res Physics Space Physics* 123:4094–4109. <https://doi.org/10.1029/2018JA025365>
- Yamazaki Y, Matthias V, Miyoshi Y, Stolle C, Siddiqui T, Kervalishvili G, Laštovička J, Kozubek M, Ward W, Themens DR, Kristoffersen S, Alken P (2020) September 2019 Antarctic Sudden Stratospheric Warming: Quasi-6-Day Wave Burst and Ionospheric Effects. *Geophys Res Lett.* <https://doi.org/10.1029/2019GL086577>
- Yue J, Wang WB (2014) Changes of thermospheric composition and ionospheric density caused by quasi 2 day wave dissipation. *J Geophysical Res Space Physics* 119:2069–2078. <https://doi.org/10.1002/2013JA019725>
- Yue J, Wang WB, Ruan HB, Chang LC, Lei JH (2016) Impact of the interaction between the quasi two-day wave and tides on ionosphere and thermosphere. *J Geophys Res Physics Space Physics* 121:3555–3563. <https://doi.org/10.1002/2016JA022444>
- Zhao B, Wan W, Liu L, Igarashi K, Nakamura M, Paxton LJ, Su SY, Li G, Ren Z (2008) Anomalous enhancement of ionospheric electron content in the Asian Australian region during a geomagnetically quiet day. *J Geophys Res* 113:A11302. <https://doi.org/10.1029/2007JA012987>

Publisher's Note

Springer Nature remains neutral with regard to jurisdictional claims in published maps and institutional affiliations.

Submit your manuscript to a SpringerOpen® journal and benefit from:

- Convenient online submission
- Rigorous peer review
- Open access: articles freely available online
- High visibility within the field
- Retaining the copyright to your article

Submit your next manuscript at ► [springeropen.com](https://www.springeropen.com)